THE JOURNAL OF PHYSICAL CHEMISTRY C

Article

Spontaneous Reduction of Pt(IV) onto the Sidewalls of Functionalized Multiwalled Carbon Nanotubes as Catalysts for Oxygen Reduction Reaction in PEMFCs

Z. D. Wei, C. Yan, Y. Tan, L. Li, C. X. Sun, Z. G. Shao, P. K. Shen, and H. W. Dong

J. Phys. Chem. C, **2008**, 112 (7), 2671-2677 • DOI: 10.1021/jp709936p

Spontaneous Reduction of Pt(IV) onto the Sidewalls of Functionalized Multiwalled Carbon Nanotubes as Catalysts for Oxygen Reduction Reaction in PEMFCs

Z. D. Wei,*,†,‡ C. Yan,‡ Y. Tan,‡ L. Li,‡,§ C. X. Sun,† Z. G. Shao,⊥ P. K. Shen,*,|| and H. W. Dong†,‡

The State Key Laboratory of Power Transmission Equipment & System Security and New Technology, Chongqing University, Chongqing 400044, China, School of Chemistry and Chemical Engineering, Chongqing University, Chongqing 400044, China, School of Material Science and Engineering, Chongqing University, Chongqing 400044, China, Dalian Institute of Chemical Physics, Chinese Academy of Sciences, Dalian 116023, China, and The State Key Laboratory of Optoelectronic Materials and Technologies, School of Physics and Engineering, Sun Yat-Sen University, Guangzhou 510275, China

Received: October 12, 2007; In Final Form: December 5, 2007

This paper reports spontaneous formation of metal nanoparticles on the sidewalls of the functionalized MCNTs (FMCNTs) when the FMCNTs were immersed in corresponding metal salt solutions. At first, MCNTs were functionalized by oxidation of a mixture consisting of H_2SO_4/HNO_3 or H_2SO_4/H_2O_2 and formed oxygen-containing functional groups such as −COOH, −OH, etc., by which the metal ions (Pt^{4+}) were reduced on the sidewalls of FMCNTs. No other substance that is suspicious of being a reducer was introduced in the Pt^{4+} ion reduction. The properties of FMCNTs and platinized FMCNTs were characterized electrochemically and instrumentally. The results showed that the electrode made from platinized FMCNTs with Pt loading of 0.12 mg cm^{-2} had enhanced catalytic activity for the oxygen reduction reaction over one made from commercial Pt/C catalyst with Pt loading of 0.27 mg cm^{-2}.

1. Introduction

One of the key requirements in making proton exchange membrane fuel cells (PEMFCs) commercially viable is to reduce the cost by reducing the amount of precious metal catalyst used. Highly dispersed nanoscale Pt particles have been an intensively researched subject as the electrocatalysts for the methanol oxidation and oxygen reduction reaction (ORR).[1−3] Much effort has been devoted to develop electrodes with high utilization of noble metal catalysts. In recent years there has been progress in understanding that the catalyst−support interaction plays a fundamental role in the performance of the catalyst. The good properties of the catalyst supports, such as high surface area and good electronic conductivity, are essential for the Pt catalyst to produce high catalytic activity. In most cases, carbon black is used as support for noble metal catalysts. However, the carbon black is easily corroded resulting in loss of catalysts, which will do harm to the performance of the cell. The solution to the corrosion problem is graphitization of carbon blacks. It is well-known that the graphitization requires a high temperature and high pressure which demand more of the equipment. In fact, the cost of the carbon black after graphitization would be as high as that of the carbon nanotubes (CNTs). Besides, it is hardly a guarantee for the full transformation of the carbon black to graphite.

CNTs as a new form of carbon have received the attention of researchers due to their unique structural, electronic, and mechanical properties.[4−7] The use of CNTs as alternative supports for the preparation of catalysts for low-temperature fuel cells has naturally stimulated significant interest among researchers. Pt has been deposited on activated single carbon nanotubes (SCNTs) and multiwalled carbon nanotubes (MCNTs) by the chemical reduction method and the resultant electrodes show good electrocatalytic activities for hydrogenation oxidation[8−11] and the ORR.[12−14] Liu et al.[13] reported the preparation of CNTs-coated Pt nanoparticles by the two-step sensitization−activation method. The Pt/CNTs exhibited high electrocatalytic activity for the ORR. Yan et al.[15] had used MCNTs as a Pt catalyst support by growing MCNTs directly on carbon paper through a chemical vapor deposition process using electrodeposited Co as the catalyst for MCNTs growth and subsequently depositing Pt catalyst selectively on these MCNTs. Yoshitake et al.[16] loaded the oxide colloid of Pt to the SCNTs and subsequently reduced Pt particles to the SCNTs using H_2 to obtain the Pt/SCNTs catalyst.

In favor of efficient catalysis on the electrodes of PEMFCs, gas molecules must be able to easily access the surface of the catalyst particles, a pathway for proton diffusion must exist in the proximity of the active sites on catalysts, and an electronic conducting pathway from the catalyst to the electrode is also required for electron transport.[17,18] For given Pt loadings, it is always expected that almost all Pt catalyst particles are effective in the electrochemical reactions. However, this is not always the case, especially in the case of perfluorosulfonete ionomer (PFSI) electrolyte used as binder, where Pt catalysts are present. When CNTs were used to substitute carbon black as support materials, the electron pathway will be greatly increased due to the wire-like structure of the CNTs. As is schematically shown in Figure 1, many carbon black particles are isolated by the dielectric organic polymer and thus the metallic catalysts

* Authors to whom correspondence should be addressed. E-mail: zdwei@cqu.edu.cn (Z.D.W.); stsspk@sysu.edu.cn (P.K.S.).
† The State Key Laboratory of Power Transmission Equipment & System Security and New Technology, Chongqing University.
‡ School of Chemistry and Chemical Engineering, Chongqing University.
§ School of Material Science and Engineering, Chongqing University.
⊥ Dalian Institute of Chemical Physics, Chinese Academy of Sciences.
|| School of Physics and Engineering, Sun Yat-Sen University.

10.1021/jp709936p CCC: $40.75
Published on Web 01/30/2008

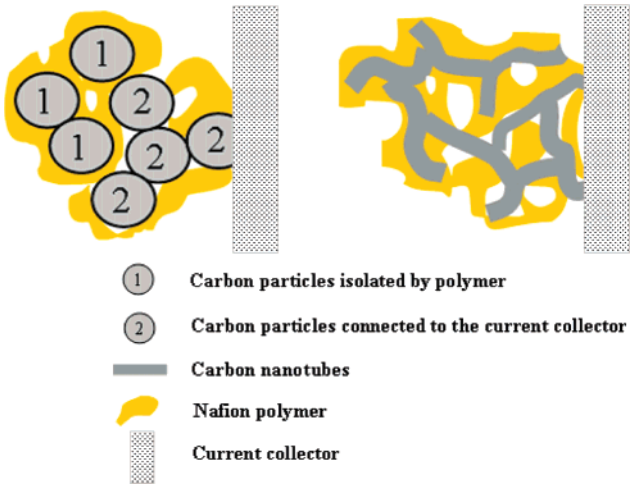

Figure 1. Schematic of the internal structure of the catalyst layer.

loaded on the carbon black particles are not going to participate in the electrode reaction because of no electron pathway. However, this may occasionally happen when using the CNTs since their tubular structure makes them easy to connect together. With the increase in the electron pathway, the number of active metallic catalysts will also increase. For example, if the probabilities of protons diffusion are 50% for the both supports and the probabilities of electron conduction are 50% for carbon black and 90% for CNTs, the utilization of active catalysts would be 25% and 45% for carbon blacks and CNTs, respectively. Using CNTs as a Pt substrate may also increase Pt utilization in addition to the feats CNTs brings to the catalyst system, good corrosion resistance and good conductance.

For the preparation of the platinum catalyst, chemical reduction methods[8,12,13,19,20] and electrodeposition methods[21,22] are commonly used. However, the impurities are easily involved from the bath solution by using chemical reduction methods, which may deteriorate the catalytic activity of the prepared catalysts. The electrodeposition method can control the metallic catalyst loading easily, but it is hardly able to control the particle size because the existing particles will serve as a new growth point and lead to particles growing bigger.

This paper reports spontaneous formation of metal nanoparticles on functionalized MCNTs (FMCNTs) sidewalls when the FMCNTs are immersed in corresponding metal salt solutions. The work is motivated by a recent observation by Choi et al.[23] that line-like metal structures with width <10 nm spontaneously deposited on SWNTs as a result of direct redox reactions between metal ions and nanotubes. The energy difference of electrons between the SCNTs and the metal ions (Au^{3+}, Pt^{4+}) was ascribed to be responsible for the electron transferring spontaneously from the SCNTs to metal ions Au^{3+} and Pt^{4+} and thus leads to the reduction of the metal ions. However, the spontaneous reduction between the SCNTs and the metal ions (Au^{3+}, Pt^{4+}) would proceed very slowly in our experiment if the metal ions solution did not contain any ethanol, which was added as a wetting reagent in Choi's work.[23] Therefore, it is difficult to eliminate ethanol from the reducers because the ethanol has a more negative potential than the SCNTs, 0.087 V[24] vs 0.5 V.[23] This means that, thermodynamically, the ethanol is a much better reducer than the SWNTs. In addition, the purpose of Choi's work was to make a line-like metal wire that was subsequently peeled off from the SCNTs. Thus, the binding strength between the metal wires and the SCNTs should be weak. In fact, the weaker, the better for metal wire peeling. However, the binding strength between the metal deposits and the SCNTs should be strong enough if they served as catalysts and catalyst supports. Otherwise, metal catalysts would run off from the supports. Generally, the binding strength between the metal deposits and the SCNTs is not strong because of the perfect graphite structure of the SCNTs. In other words, there are not enough suspending bonds or unsaturated bonds on the wall of SCNTs left for foreign substances to bond. Thus, making defects on the walls of MCNTs is one task of this work in order to produce some suspending bonds or unsaturated bonds for anchoring Pt catalysts. It has been widely believed that CNTs can be functionalized by oxidation of a mixture consisting of H_2SO_4/HNO_3 or H_2SO_4/H_2O_2 and form the oxygen-containing functional groups, such as −COOH, −OH, etc.[25] The more intensely the oxidation carries on, the more oxygen-containing functional groups would be introduced on the walls of MCNTs. The oxygen-containing functional groups make the CNTs hydrophilic, and make it possible for an efficient reduction of metal ions (Pt^{4+}) by the introduced groups −COOH, −OH, and electrons from FMCNTs themselves. No substance that is likely suspicious of being a reducer was introduced in the Pt ion reduction. Meanwhile, we also expect that the oxygen-containing functional groups play a role in anchoring Pt particles on the walls of FMCNTs.

2. Experimental Section

The raw MCNTs (rMCNTs) were purchased from Shenzhen Bill Technological Development Lt. Co. with the diameters of 20−40 nm, lengths of 3−18 μm, and purity of 95%.

2.1. Purification and Functionalization of rMCNTs. The rMCNTs were purified by boiling in 14 mol/L HNO_3 for 5 h, then diluted with water, filtered, and finally washed with excess deionized (DI) water and ethanol in that order. The purified MCNTs (pMCNTs) were dried at 100 °C in an oven. The functionalization of pMCNTs was carried out in H_2SO_4/H_2O_2 solution (4:1 by volume) for 0.5 h. The functionalized MCNTs (FMCNTs) were diluted with water and filtered, then washed with excess DI water and ethanol in that order. Finally the FMCNTs were dried at about 100 °C for future use.

2.2. Preparation of Teflon-Boned Carbon Black Electrodes (TBCE). The Teflon-boned carbon electrodes (TBCE) were prepared as described previously.[17] In short, the electrode was composed of a gas diffusion layer and a catalyst layer. The gas diffusion layer was prepared on wet-proofed carbon paper. The carbon powder (Vulcan XC-72, Cabot Corp.), 30 wt % of Teflon, and ethanol were ultrasonically mixed with a 1:1 ratio of carbon to solid Teflon loading. The viscous mixture was coated onto the carbon paper (Tony Co, Jap.) wet-proofed by Teflon and then heated at 340 °C for 30 min. The loading of carbon powder is 1.0 mg/cm^2.

2.3. Loading Platinum onto the FMCNTs by Spontaneous Reduction. The platinum particles were loaded onto the FMCNTs in two ways. Pt was spontaneously reduced on the FMCNTs after or before FMCNTs was coated on the TBCE. Accordingly, the electrodes prepared in these two ways are named 1-Pt/FMCNTs and 2-Pt/FMCNTs, respectively. The procedure details in the preparation of 1-Pt/FMCNTs and 2-Pt/FMCNTs are summarized as follows.

(*1*) *1-Pt/FMCNTs*: After the preparation of TBCE, the hydrophilic ink containing FMCNTs and 0.5% Nafion with a 1:25 dry weight ratio of Nafion to FMCNTs as well as ethanol was coated on the TBCE and then dried at 145 °C for 0.5 h. The above electrode-coated FMCNTs was immersed in 3 mmol/L K_2PtCl_4 solution at 40−45 °C for 48 h. The pH value

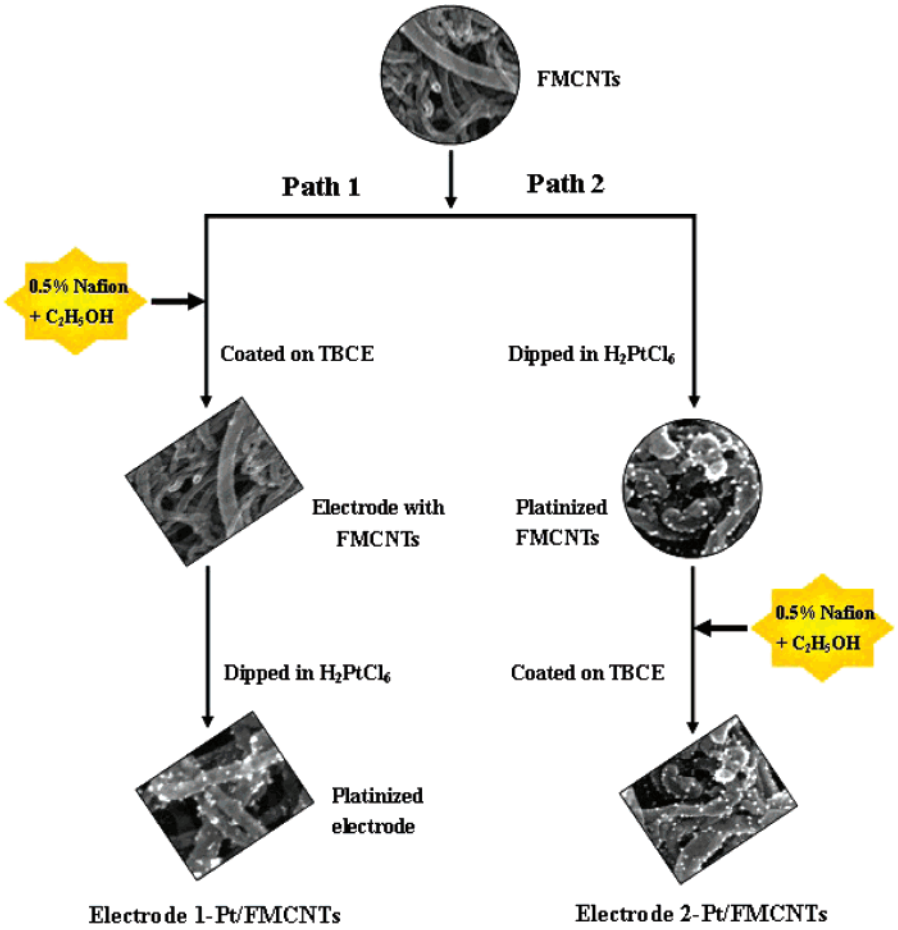

Figure 2. Schematic diagram for preparing Pt/FMCNTs electrodes.

was adjusted to 8 by adding of KOH solution. Finally the electrode was obtained after being rinsed with copious amounts of water.

(*2*) *2-Pt/FMCNTs*: The FMCNTs were ultrasonically dispersed in 3 mmol/L K_2PtCl_4 solution at 40−45 °C for 48 h. The pH value was adjusted to 8 by adding KOH solution. The mixture was filtered and washed with excess DI water and ethanol in that order. The Pt/FMCNTs catalysts were finally obtained. The hydrophilic ink containing Pt/FMCNTs and 0.5% Nafion with the 1:25 dry weight ratio of Nafion to FMCNTs as well as ethanol was coated on the TBCE and then dried at 145 °C for 0.5 h.

It was expected that 1-Pt/FMCNTs has higher Pt utilization than 2-Pt/FMCNTs because Pt is reduced only on the exposed functionalized groups. The procedure in the preparation of 1-Pt/FMCNTs and 2-Pt/FMCNTs was demonstrated in Figure 2.

2.4. Characterization of Pt/FMCNTs Electrodes. All electrochemical experiments were performed in a three-electrode cell at room temperature. The working electrode was Pt/FMCNTs prepared in this work, and a Pt wire and a saturated potassium chloride silver chloride electrode (SSCE) (0.20 V vs SHE) were employed as a counter electrode and a reference electrode, respectively. All potentials are quoted with respect to the SSCE reference electrode unless otherwise stated. Linear-sweep Voltammetry (LSV) and Cyclic Voltammetry (CV) were employed to characterize Pt/FMCNTs prepared by spontaneous reduction. The Nafion-bonded Johnson-Matthey Pt/C catalysts electrode was used for comparison and named electrode JM-Pt/C hereafter.

The XRD measurement was carried out on SHIMADIU XRD-6000 (Japan). Cu Ka (k = 0.15418 nm) serves as the radiation source. The X-ray diffraction spectra were obtained at a scan rate of 4 deg/min in a range of 2θ from 30° to 80°. The theoretical average particle size was estimated by using the Scherrer formula.[26] Although there are several XRD peaks that can be used for estimation of the particle size, only the width at half-height corresponding to the (110) plane at 2θ = 39.7° was used to determine the average Pt particle size because the data at a low diffraction angle would lead to error in estimation of particle size compared with those at a high angle according to the literature.[27] SEM images of the pMCNTs and Pt/FMCNTs were obtained from an FEI Nova 400 nona field emission scanning electron microscope (FESEM) from Netherland (Peabody, MA). FTIR images of the MCNTs and Pt/MCNTs were obtained from a MAGNA-IR 550 spectrometer series II (Nicolet Co.).

Spectrophotometry with a color-developing agent of $SnCl_2$ was used to determine the Pt content of Pt/MCNTs.[28] First, the tested electrode was calcinated in air at a temperature of 700−800 °C to remove the carbon carrier and polymer, then the residue was dissolved in aqua regia to form a Pt ion containing solution, in which 4 mL of 37% HCl, 5 mL of 20% NH_4Cl, and 2.5 mL of 20% $SnCl_2$ hydrochloric acid solution (the volume ratio of HCl to water is 1:1) were added. Finally, Pt content was determined on a spectrophotometer (TU-1900/TU-1901, Beijing PuXi, China) by measuring the absorbency of the platinum containing solution at a wavelength of 403 nm.

3. Results and Discussion

3.1. Characterization of the FMCNTs. Figure 3 shows the morphological images of rMCNTs and pMCNTs. It can be seen

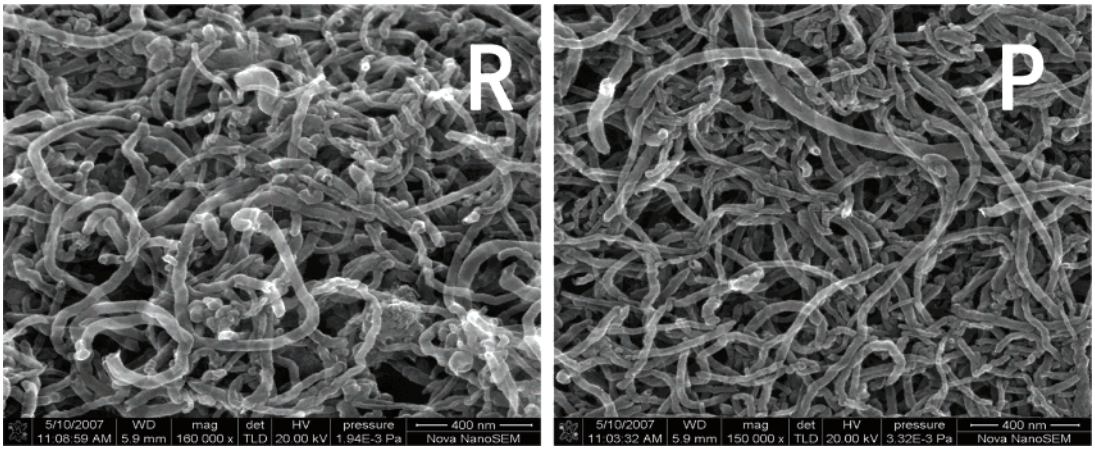

Figure 3. SEM images of rMCNTs (R) and pMCNTs (P).

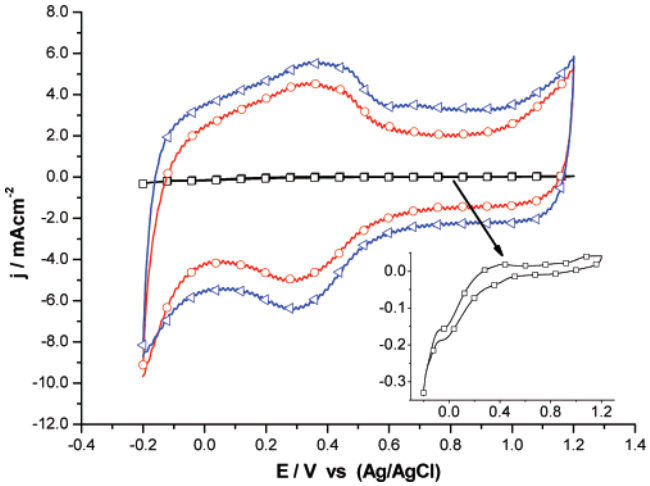

Figure 4. CV curves of electrodes made from rMCNTs (square), pMCNTs (circle), and FMCNTs (triangle) in 0.5 mol/L H_2SO_4. The loading of MCNTs is 2.5 mg/cm^2 and the scan rate is 50 mV/s.

that the impurity and metal catalyst which were introduced in fabrication of MCNTs were markedly reduced and the intertwist between MCNTs was opened after the purification. The image of pMCNTs appears cleaner than that of rMCNTs.

Figure 4 shows the CV curves of electrodes made from rMCNT, pMCNTs, and FMCNTs in 0.5 mol/L H_2SO_4, and the inset is the magnified CV curve of the electrode made from rMCNT. It can be seen that there are redox peaks at around 0.3 and 0.4 V in CV curves of electrodes made from pMCNTs and FMCNTs, which correspond to the reduction/oxidation peaks of carboxyl. This indicates that the carboxyl has been successfully introduced into the walls of pMCNTs and FMCNTs after purification and fuctionalization. The difference in a redox potential between 0.3 V of carboxyl redox potential and 0.57 V of Pt^{4+} redox potential[23] is the electrochemical motive force (EMF) for Pt^{4+} reduction. Such an EMF with a value of 0.27 V seems not large enough to facilitate the redox reaction quickly. This is why the spontaneous reaction process requires as long as 48 h. Besides, in comparison with the extremely narrow CV curves of the electrode made from rMCNTs, the markedly increased width of the CV curves of the electrodes made from pMCNTs and FMCNTs suggests that the area of the electrode/electrolyte interface was continuously enhanced after purification and fuctionalization step by step. In other words, the hydrophlicity of the electrodes has been improved markedly with purification and fictionalization.

In addition, the redox peaks between 0.3 and 0.4V were also attributed to the redox of quinone−hydroquinone.[29,30] According to our understanding, carboxyl groups and quinone−hydroquinone are two expressions of the same substance in the environment of the FMWCNs. Even though there is some difference between them, such difference is not great at all. Carboxyl groups and quinone−hydroquinone most likely reduce/oxide at the very close potential. They both have the capability of reducing Pt ions.

3.2. Characterization of the Pt/FMCNTs. Figure 5 shows the SEM images of electrodes 1-Pt/FMCNTs and 2-Pt/FMCNTs. SEM images showed that Pt nanoparticles with a narrow particle size distribution are uniformly dispersed on both electrodes. Compared with the image of electrode 1-Pt/FMCNTs, a slight particle agglomeration can be observed in the image of electrode 2-Pt/FMCNTs as marked by circles 1 and 2 in Figure 5. The XRD spectra of electrodes 1-Pt/FMCNTs and 2-Pt/FMCNTs are shown in Figure 6. The mean nanoparticle size (diameter) estimated by Scherrer's formula[26] is about 5.0 nm for both electrodes. The uniformly dispersed Pt particles in SEM images of Figure 5 further proved our early analysis in the introduction to be correct, that is, Pt^{4+} ions were mainly reduced by carboxyl groups, which were successively generated in purification and fictionalization and highly dispersed on the walls of the FMCNTs. If the Pt^{4+} ions reductions were directly by the electrons from the walls of the FMCNTs, the reduced Pt deposits should cover the whole surface of the FMCNTs walls rather than be dispersed in a speck-like distribution on the walls of the FMCNTs. The wire-like Pt deposits in Choi's work[23] were probably the result of co-reduction of existing carboxyl groups on the wall of the SCNTs and the ethanol in the Pt^{4+} ions solution. The former produced a growth point of the Pt wire; the later facilitated the growth of the Pt wire.

The FTIR spectra of rMCNTs, pMCNTs, FMCNTs, and Pt/FMCNTs are presented in Figure 7. The band at 1632 cm^{-1} is a characteristic peak of carbon materials.[31] The bands at 1729 and 1578 cm^{-1} are ascribable to carbonyl groups C═O in the carboxylic acid group and aroma group, respectively.[32] The CNTs was composed of a five-carbon-atom circle or a six-carbon-atom circle, which is similar to the aroma group, so the band at 1578 cm^{-1} can be ascribed to the typical features of CNTs.[25] It is clear that the band at 1729 cm^{-1} gradually increases from rMCNTs to pMCNTs and finally to FMCNTs. This implies that the carboxylic acid group was successively produced in purification and functionalization. This is coincident to the analysis mentioned in the discussion of Figure 4. The decrease in intensity of the carboxylic acid band at 1729 cm^{-1}

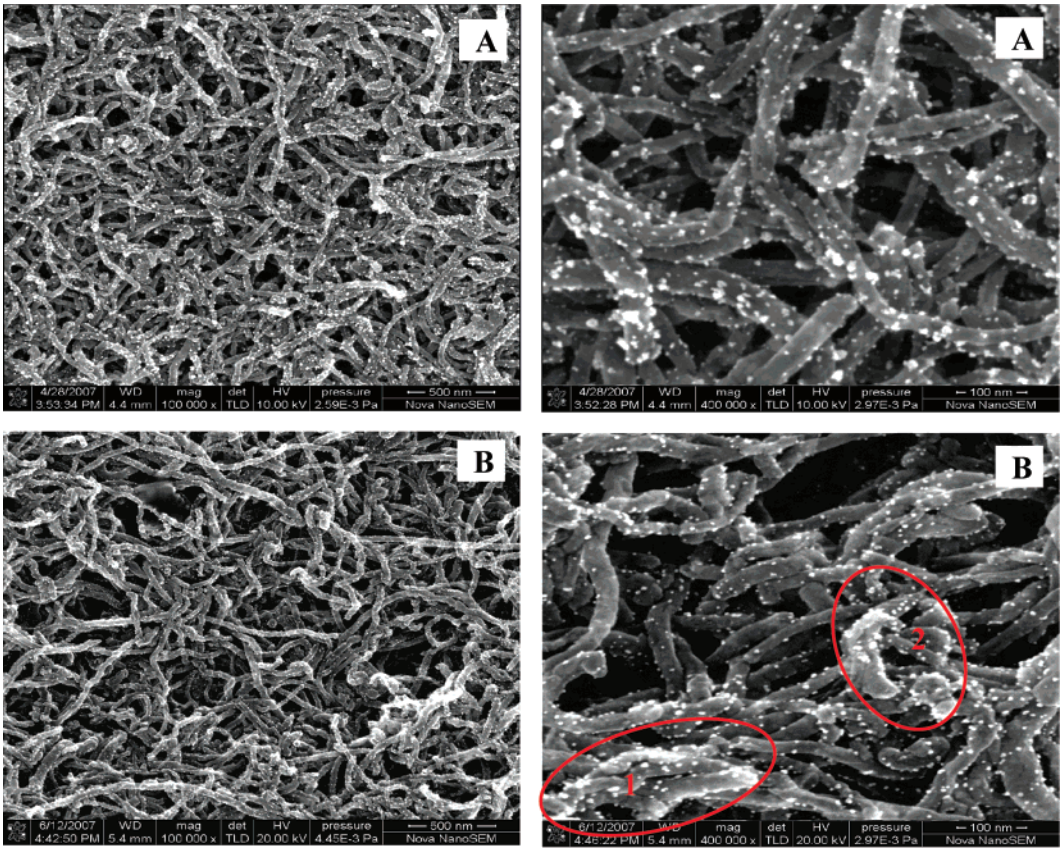

Figure 5. SEM images of electrodes 1-Pt/FMCNTs (A) and 2-Pt/FMCNTs (B).

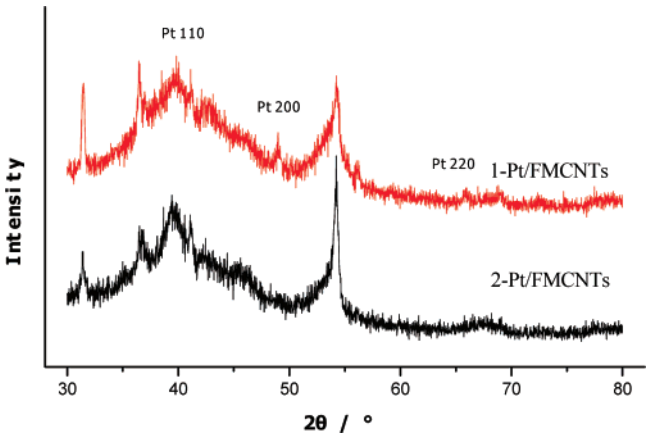

Figure 6. XRD spectra of electrode Pt/FMCNTs.

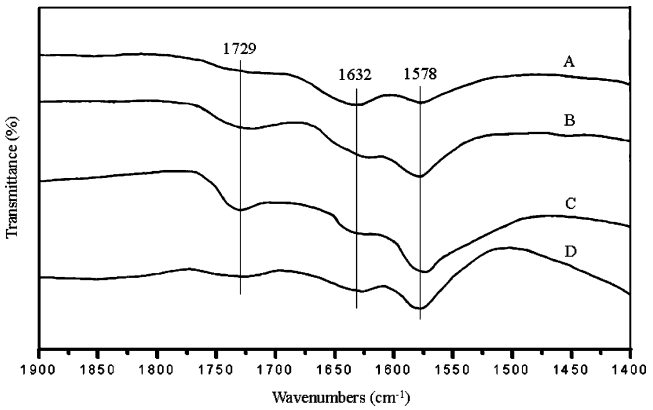

Figure 7. FTIR spectra of rMCNTs (A), pMCNTs (B), FMCNTs (C), and Pt/FMCNTs (D).

after FMCNTs transforming to Pt/FMCNTs indicates the consumption of the carboxylic groups for Pt^{4+} ions reduction.

The CV curves of electrodes 1-Pt/FMCNTs and 2-Pt/FMCNTs are shown in Figure 8 together with the CV curve of electrode JM-Pt/C for comparison. The smaller electrochemical surface area (ECSA) of electrode 2-Pt/FMCNTs indicated by the area of hydrogen desorption/adsorption in the CV can be ascribed to the loss in Pt active sites due to Pt/FMCNTs embedded inside the electrode after Pt/FMCNTs was coated on the TBCE. This situation did not happen in the preparation of electrode 1-Pt/FMCNTs, where Pt particles only deposit on the sites open to the Pt ion solution. The same Pt/C particle embedding happens in the case of electrode JM-Pt/C. This shortcoming, however, was compensated for by the large specific area of JM-Pt/C catalysts due to their very small particle size. In addition, the Pt loading of electrode JM-Pt/C in Figure 8 is also the highest of the three electrodes. These all lead to electrode JM-Pt/C having a middle value of ECSA among the three electrodes.

ECSA is an important factor in assessing the performance of electrodes. The higher ECSA, the more electrochemical active sites would exist. The ECSA of an electrode was estimated by calculating the average value of hydrogen desorption/adsorption charges according to formula 1[33]

$$A = \frac{Q_H}{[Pt] \times 0.21} \quad (1)$$

where A refers to the ECSA (cm^2/mg), Q_H represents for the average value of the hydrogen desorption/adsorption charges (mC/cm^2), [Pt] is the Pt loadings (mg/cm^2), and 0.21 (mC/cm^2) is the value of Q_H per square centimeter of Pt. The estimated ECSA of electrodes 1-Pt/FMCNTs, 2-Pt/FMCNTs, and JM-Pt/C according to the CV curves of Figure 8 is 423.8, 250.2, and 366.8 cm^2/mg, respectively.

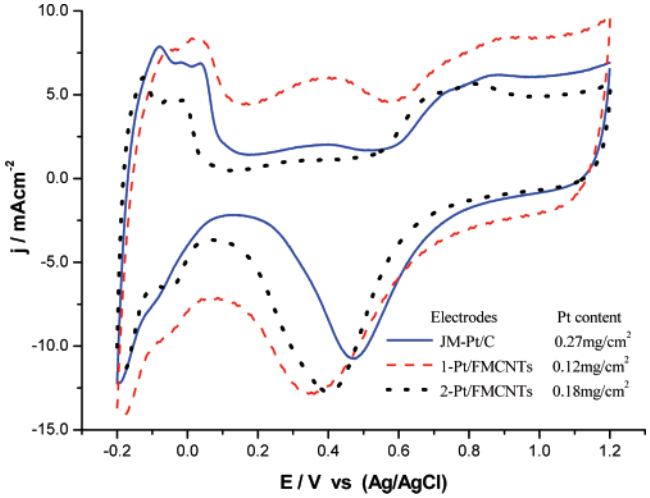

Figure 8. CV curves of electrodes 1-Pt/FMCNTs, 2-Pt/FMCNTs, and JM-Pt/C in 0.5 mol/L H_2SO_4 at 50 mV/s.

TABLE 1. Information Obtained from the Figures

electrodes	Pt content (mg/cm^2)	$D_{(XRD)}$ (nm)	ECSA (cm^2/mg)	utilization (%)
JM-Pt/C	0.27	3.0	366.8	39.2
1-Pt/FMCNTs	0.12	5.0	423.8	75.6
2-Pt/FMCNTs	0.18	5.0	250.2	44.6

The utilization of Pt in the electrodes was estimated by formula 2, in which μ is the utilization, A is ECSA, and S is the total surface area per volume of particle.[33]

$$\mu = \frac{A}{S} \tag{2}$$

S (cm^2/mg) is calculated by formula 3,[34] in which $\rho = 2.14 \times 10^4$ mg/cm^3 is the density of platinum and d (cm) the Pt diameter calculated by XRD spectra.

$$S = \frac{60}{\rho d} \tag{3}$$

Thus, we obtained the utilization of Pt in electrodes 1-Pt/FMCNTs, 2-Pt/FMCNTs, and JM-Pt/C as 75.6%, 44.6%, and 39.2% respectively. For the sake of convenient comparison, the data associated with the three electrodes are summarized in Table 1. Electrodes 2-Pt/FMCNTs and JM-Pt/C were fabricated by almost the same procedure, but the former has a 5.4% Pt utilization higher than the later. There is no other account but electrode 2-Pt/FMCNTs having a much better-connected electron path contributed by the FMCNTs than the JM-Pt/C electrode.

3.3. Behavior of the Electrodes for the ORR. Linear-sweep Voltammetry (LSV) was employed to assess the catalytic capability of electrodes 1-Pt/FMCNTs, 2-Pt/FMCNTs, and JM-Pt/C for the ORR. The results are shown in Figure 9. Although electrode 1-Pt/FMCNTs has the lowest Pt content of three electrodes, it exhibits the best catalytic activity toward the ORR. The performance of electrode 2-Pt/FMCNTs is also better than that of electrode JM-Pt/C. The higher catalytic activities for the ORR of electrodes 1-Pt/FMCNTs and 2-Pt/FMCNTs are obviously due to their higher Pt utilization, which results on the one hand primarily from the well-connected electron path contributed by the FMCNTs and on the other hand likely from the assistant catalytic function of functionalized MCNTs. In addition, the current produced by the direct reduction of the carboxyl groups on FMCNTs after 0.6 V as illustrated in Figure 4 also contributes to the current increase in the ORR.

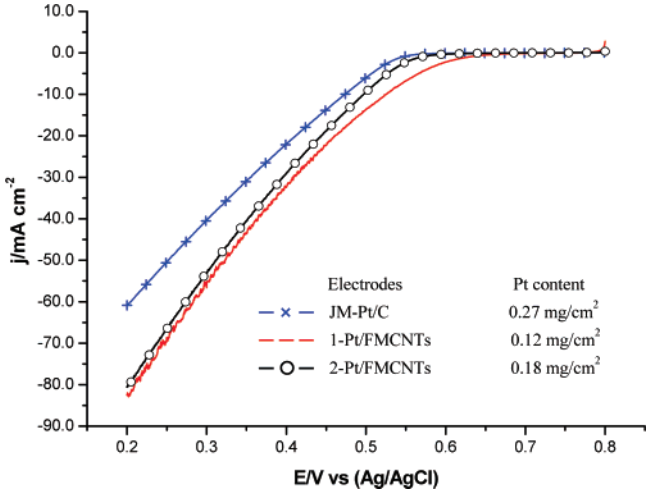

Figure 9. Polarization curves of electrodes 1-Pt/FMCNTs, 2-Pt/FMCNTs, and JM-Pt/C in oxygen-saturated 0.5 mol/L H_2SO_4 at 2 mV/s.

4. Conclusions

The electrodes 1-Pt/FMCNTs and 2-Pt/FMCNTs prepared by spontaneous reduction deposition exhibit higher electrochemical activity for the ORR. Pt nanoparticles were uniformly dispersed on the active sites of FMCNTs. The functionalization to FMCNTs in a mixture consisting of H_2SO_4/HNO_3 or H_2SO_4/H_2O_2 can produce oxygen-containing functional groups on the walls of FMCNTs, such as −COOH, −OH, etc., which make the CNTs hydrophilic and make it possible for an efficient reduction of Pt^{4+} ions. It is proposed that the oxygen-containing functional groups also play a role in anchoring Pt particles on the walls of FMCNTs. The FIRT spectra indicated that the −COOH groups of FMCNTs play a reducing role in Pt deposition. The higher catalytic activities toward the ORR of electrodes 1-Pt/FMCNTs and 2-Pt/FMCNTs are obviously due to their higher Pt utilization, which on one hand results primarily from the well-connected electron path contributed by the FMCNTs and on the other hand likely from the assistant catalytic function of functionalized MCNTs. In addition, the current produced by the direct reduction of the carboxyl groups on FMCNTs after 0.6 V also contributes to the current increase in the ORR.

Acknowledgment. This work was financially supported by NSFC of China (Grant Nos. 20476108, 20476109, and 20676156), the Chinese Ministry of Education (Grant Nos. NCET-04-0850 and 307021), the China National 863 Program (Grant Nos. 2006AA11A141 and 2007AA05Z124), the Guangdong Sci&Tech Key Project (Grant No. 2007A010700001), and the Chongqing Sci&Tech Key Project (Grant No. CSTC2007AB6012).

References and Notes

(1) Morris, C. A.; Anderson, M. L.; Stroud, R. M.; Merzbacher, C. I.; Rolison, D. R. *Science* **1999**, *284*, 622.
(2) Tong, Y.; Rice, A.; Wieckowski, A.; Oldfield, E. *J. Am. Chem. Soc.* **2000**, *122*, 1123.
(3) Cui, H. F.; Ye, J. S.; Zhang, W. D.; Wang, J.; Sheu, F. S. *J. Electroanal. Chem.* **2005**, *577*, 295.
(4) Baughman, R. H.; Zakhidov, A. A.; Heer, W. A. *Science* **2002**, *297*, 787.
(5) Che, G.; Lakshmi, B. B.; Martin, C. R.; Fisher, E. R. *Langmuir* **1999**, *15*, 750.

(6) Wilder, J. W. G.; Venema, L. C.; Rinzler, A. G.; Smalley, R. E.; Dekker, C. *Nature* **1998**, *391*, 59.

(7) Kong, J.; Franklin, N. R.; Zhou, C.; Chapline, M. G.; Peng, S.; Cho, K.; Dai, H. *Science* **2000**, *287*, 622.

(8) Lordi, V.; Yao, N.; Wei, J. *Chem. Mater.* **2001**, *13*, 733.

(9) Huang, J. E.; Guo, D. J.; Yao, Y. G.; Li, H. L. *J. Electroanal. Chem.* **2005**, *577*, 93.

(10) Wu, G.; Chen, Y. S.; Xu, B. Q. *Electrochem. Commun.* **2005**, *7*, 1237.

(11) Chen, W. X.; Zhao, J.; Jim, Y. L.; Liu, Z. L. *Mater. Chem. Phys.* **2005**, *91*, 124.

(12) Li, W. Z.; Liang, C. H.; Qiu, J. S.; Zhou, W. J.; Han, H. M.; Wei, Z. B.; Sun, G. Q.; Xin, Q. *Carbon* **2002**, *40*, 791.

(13) Liu, Z. L.; Lin, X. H.; Lee, J. Y.; Zhang, W. D.; Han, M.; Gan, L. M. *Langmuir* **2002**, *18*, 4054.

(14) Rajalakshmi, N.; Ryu, H.; Shaijumon, M. M.; Ramaprabhu, S. *J. Power Sources* **2005**, *140*, 250.

(15) Wang, C.; Waje, M.; Wang, X.; Tang, J. M.; Haddon, R. C.; Yan, Y. S. *Nano Lett.* **2004**, *4*, 345.

(16) Yoshitake, T.; Shimakawa, Y.; Kuroshima, S.; Kimura, H.; Ichihashi, T.; Kubo, Y.; Kasuya, D.; Takahashi, K.; Kokai, F.; Yudasaka, M.; Iijima, S. *J. Phys. B* **2002**, *323*, 124.

(17) Wei, Z. D.; Chen, S. G.; Liu, Y.; Sun, C. X.; Shao, Z. G.; Shen, P. K. *J. Phys. Chem. C* **2007**, *111*, 15456.

(18) Wei, Z. D.; Chan, S. H. *J. Electroanal. Chem.* **2004**, *569*, 23.

(19) Yu, R. Q.; Chen, L. W.; Liu, Q. P.; Lin, J. Y.; Tan, K. L.; Ng, S. C.; Chan, H. S. O.; Xu, G. Q.; Andy Hor, T. S. *Chem. Mater.* **1998**, *10*, 718.

(20) Yoo, E.; Nagashima, Y.; Yamazaki, T.; Matsumoto, T.; Nakamura, J. *Polym. Adv. Technol.* **2006**, *17*, 540.

(21) Goodenough, J. B.; Hamnett, A.; Kennedy, B. J.; Manoharan, R.; Weeks, S. A. *Electrochim. Acta* **1990**, *35*, 199.

(22) Tang, H.; Chen, J. H.; Huang, Z. P.; Wang, D. Z.; Ren, Z. F.; Nie, L. H.; Kuang, Y. F.; Yao, S. Z. *Carbon* **2004**, *42*, 191.

(23) Choi, H. C.; Shim, M.; Bangsaruntip, S.; Dai, H. J. *J. Am. Chem. Soc.* **2002**, *124*, 9085.

(24) Zhao, X. S.; Jiang, L. H.; Sun, G. Q.; Yang, S. H.; Yi, B. L.; Xin, Q. *Chin. J. Catal.* **2004**, *25*, 983.

(25) Li, X. H.; Niu, J. L.; Zhang, J.; Li, H. L.; Liu, Z. F. *J. Phys. Chem. B* **2003**, *107*, 2453.

(26) Ioroi, T.; Kitazwa, N.; Yasuda, K.; Yamamoto, Y.; Takenaka, H. *J. Appl. Electrochem.* **2001**, *31*, 1179.

(27) Zhou, G. D.; Duan, L. Y. *Structure Chemistry*; Peking University Press: Beijing, China, 1995; Vol. II, p 378.

(28) Cai, S. X.; Huang, C. *Noble metal analysis*; Metallurgical Industry Press: Beijing, China, 1984; p 199.

(29) Kangasniemi, K. H.; Condit, D. A.; Jarvi, T. D. *J. Electrochem. Soc.* **2004**, *151* (4), E125.

(30) Shao, Y. Y.; Yin, G. P.; Zang, J.; Gao, Y. Z. *Electrochim. Acta* **2006**, *51* (26), 5853.

(31) Shao, Y. Y.; Yin, G. P.; Wang, J. J.; Gao, Y. Z.; Shi, P. F. *J. Electrochem. Soc.* **2006**, *153*, A1261.

(32) Liu, M. X.; Luo, G. A.; Zhang, X. R.; Tong, A. J. *Instrumental methods of analysis*; Peking University Press: Beijing, China, 2002; Vol. II, p 157.

(33) Pozio, A.; De Francesco, M.; Cemmi, A.; Cardellini, F.; Giorgi, L. *J. Power Source* **2002**, *105*, 13.

(34) Stonehart, P. *J. Appl. Electrochem.* **1992**, *22*, 995.